Plasmonics (2023) 18:577–585
https://doi.org/10.1007/s11468-022-01761-1

Numerical Analysis of Coronavirus Detection Using Photonic Crystal Fibre–Based SPR Sensor

Ankur Gupta[1,2] · Tanu Singh[2] · Rajat Kumar Singh[1] · Akhilesh Tiwari[2]

Received: 5 November 2022 / Accepted: 1 December 2022 / Published online: 24 January 2023

Abstract

Coronavirus disease (COVID-19) is a worldwide health emergency caused by the coronavirus 2 (severe acute respiratory illness) (SARS-CoV-2). COVID-19 has a wide range of symptoms, making a definitive diagnosis difficult. The shortage of equipment for testing technology COVID-19 has resulted in long queues for COVID-19 testing, which is a major problem. COVID-19 testing is currently performed using sluggish and costly technology like single-photon emission computed tomography (SPECT), computed tomography (CT), positron emission tomography (PET), and enzyme-linked immunosorbent assay (ELISA). The gold standard test for diagnosing COVID-19 is real-time reverse transcriptase-polymerase chain reaction (RT-PCR), which necessitates highly skilled workers and has a lengthy turnaround time. However, rapid and affordable immunodiagnostic techniques (antigen or antibody tests) are also available with some trade off accuracy. Optical sensors are frequently employed in a variety of applications, because of their increased sensitivity, strong selectivity, rapid reaction times, and outstanding resolution. The use of photonic crystal fibre (PCF) is advantageous for the quick detection of the new coronavirus and is suggested with the use of a PCF-based (Au/BaTiO3/graphene) multilayered surface plasmon resonance (SPR) biosensor. The proposed sensor can quickly detect the COVID-19 virus in two different ligand-analyte environments: (i) the virus spike receptor-binding domain (RBD) as an analyte and monoclonal antibodies (mAbs) as a probe ligand, and (ii) monoclonal antibodies (IgG or IgM) as an analyte and the virus spike RBD as a probe ligand. The finite element method (FEM) is used to quantitatively examine the performance of the PCF-based multilayered SPR sensor.

Keywords Photonic crystal fibre · Surface plasmon resonance · SPR sensors · Finite element method · Coronavirus detection

Introduction

Severe acute respiratory syndrome coronavirus-2 causes COVID-19, a contagious illness (SARS-CoV-2). COVID-19 was initially discovered in Wuhan, China, in 2019, and the disease quickly spread over the world resulting in the COVID-19 pandemic [1, 2]. On 30 January 2020, the World Health Organization labelled the novel coronavirus (COVID-19) outbreak a Public Health Emergency of International Concern, and on 11 March 2020, it was declared a global pandemic [3]. Millions of people have been afflicted, many have died, and the economies of many nations have come to a standstill since the COVID-19 outbreak in Wuhan in early December 2019 [4].

Viruses can be transmitted by inhaling, through aerosol particles, and direct contact with abiotic surfaces. SARS-CoV-2 has been discovered in faeces samples, and also there is an evidence of viral transmission via faeces. The rate of transmission of SARS-CoV-2 is greater than that of the coronavirus causing the severe acute respiratory syndrome (SARS) and the Middle East respiratory syndrome (MERS) in 2002 and 2012, respectively. Up to 12 May 2022, there have been more than 519,396,816 confirmed COVID-19 cases globally, with 6,283,131 associated deaths. SARS-CoV-2 virus proliferates rapidly in body tissues and induces the immune system. The World Health Organization has

✉ Akhilesh Tiwari
atiwari@iiita.ac.in

[1] Fiber Optics Sensors Research Lab, Department of Electronics and Communication Engineering, Indian Institute of Information Technology Allahabad, Devghat, Jhalwa, Prayagraj 211015, UP, India

[2] Modeling and Simulation Laboratory, Department of Applied Sciences, Indian Institute of Information Technology Allahabad, Devghat, Jhalwa, Prayagraj 211015, UP, India

advised scientists to conduct a large number of diagnostic tests in order to stop the virus from spreading. The testing is a crucial tool for understanding the outbreak's epidemiology. Fast diagnostic testing is critical for making timely decisions on how to treat and isolate affected individuals, which can help to reduce the spread of infectious illness [5].

The RNA genome of SARS-CoV-2 virus is positive, which expresses open reading frames (ORF) coding for structural and non-structural proteins. Spike protein (S), nucleocapsid protein (N), membrane protein (M), and envelope protein (E) come among the structural proteins of SARS-CoV-2. S protein's S_1 subunit enhances angiotensin converting enzyme-2 mediated viral attachment whereas S_2 subunit aids in fusion of membrane. The N terminal domain (NTD) and the C terminal domain (CTD) in the N protein are involved in the entrance of virus and post entry processing. Nucleocapsid formation is aided by CTD. The E protein's NTD and CTD interact to form viroporins, which are necessary for assembly of viruses. The NTD and CTD of M protein encourage the spikes integration, and its interaction with E protein aids virion formation. COVID-19 tests are divided into three categories. The genetic material of the coronavirus is detected via molecular testing (also known as PCR tests). Coronavirus proteins are detected via antigen testing and the antibody testing looks for antibodies that your immune system made in response to a past COVID-19 infection. Antibody testing cannot be utilised to determine whether or not a COVID-19 infection is active. In the reverse transcription-polymerase chain reaction (RT-PCR) technique, the outcome takes almost 1–3 days (real-time test 4 h). The RT-PCR is the gold standard for detecting viral infections like COVID-19 and Ebola. It is a laboratory test that amplifies a small amount of genetic material from a pathogen, such as RNA, from a virus. The extraction of RNA from a virus in the RT-PCR method is a time-consuming and laborious procedure [4, 6]. Although it is very accurate, this lab test necessitates highly skilled workers and has a lengthy turnaround time. However, rapid and affordable immunodiagnostic techniques (antigen or antibody tests) are available; they are not as accurate as the RT-PCR test but these biosensors have the potential to be a viable alternative to these fast point of care (POC) diagnostics [7].

Biosensors are analytical devices that combine biological recognition molecules like enzymes, antibodies, or nucleic acids with a transducer that converts the changes in the biosensing element to an electrical signal. Furthermore, this signal may be amplified to process the electrical signal and digitise the output. Biosensors are well-known for their use in medical diagnosis, environmental monitoring, food, water, and agricultural product processing [7]. There are four types of biosensors, depending on the technology used: optical biosensors, electrochemical biosensors, piezoelectric biosensors, and thermal biosensors. Optical biosensors were used to MERS virus with recognition element spike protein S_1 [8]. Surface plasmon resonance (SPR) is a phenomena generated by incident electro-magnetic waves causing free electron oscillation on metal-dielectric interface [9]. Due to their high sensitivity in detecting diverse biological and chemical components, the SPR fibre sensors have become a popular research area in recent years. They have a wide range of applications in biomedical and life security domains. The SPR is a widely used technique for studying protein-protein interactions in quantitative detail, as well as determining their equilibrium and kinetic parameters. Also, SPR is an effective tool for investigating protein-protein interactions in real time without using labels. The immobilisation of a ligand on the surface of a sensor chip linked to a gold surface is used in SPR-based binding approach. The desired ligand is immobilised on the surface of sensor chip enabling varied concentrations of analyte to flow across it and describe their interactions with the immobilised ligand. The evanescent wave generated due to total internal reflection (TIR) spreads across the metal layer at metal and dielectric medium interface excites the surface plasmon wave. The SPR signal is generated by changes in the refractive index at the gold sensor chip surface providing a change in response which can be detected when the mass associated with a binding event induces a corresponding rise in the refractive index. When the analyte flow in a microfluidic channel attaches to the immobilised ligand and rises in density at the sensor chip, these changes are recorded as variations in the resonance angle of refracted light. When the angle is reached to a definite value (resonance), the majority of the light gets transformed in SPW energy, which results in a substantial decrease in energy of the reflected light and the occurrence of reflection spectrum's resonance peak. At this point, the wavelength which is incident is referred to as SPR resonance wavelength. Resonance units (RU) are used to measure the response signal, which indicates a change in the resonance angle. A sensorgram is a plot of the binding response (RU) vs time that allows distinct stages of a binding event to be viewed and analysed by monitoring the change in the SPR signal over time [10].

Photonic crystal fibres are structures which are circular in shape and those are made of silica and have uniform and intermittent array of air gaps which are spread along the complete length and have a missing air opening at the centre. In customary PCFs, the light has been directed in its centre and is conceivable which is a result of defect centre and the air-openings in the cladding. Since the refractive index is kept higher of the centre than the cladding, the light is propagated through the centre by TIR (total internal reflection) in a similar like in any ordinary optical fibre [11, 12].

SPR is a promising optical method with sensing applications in a variety of industries, prism was initially used to induce surface plasmons [10]. Optical fibre has substituted sensors based on prism because of prism's large size and inability

to be used as remote sensing. Various research investigations in SPR-based optical fibre sensors have been conducted due to the benefits of optical fibre over prism [13]. Two major obstacles in constructing the fibre optic-based SPR sensor are phase matching between plasmonic mode and core mode, as well as packaging a microfluidics setup with waveguide and a metallic layer into a sensor, and using PCF-based SPR sensors, these issues can be solved [14, 15]. It is difficult to deposit metallic layers inside the fibre; D-shape fibres are introduced with deposition of metallic layer on D-shape [16–18].

In ref. [19], a multi-layered comprising of BK7,WS2,Au,BaTiO3 and graphene-based surface plasmon resonance (SPR) biosensor is presented for the early COVID-19 diagnosis. The interaction of different concentration of ligand and analytes changes the sensor's surface plasmon polaritons (SPPs) and the detecting area RI. The suggested sensor can quickly detect the SARS-CoV-2 ligand-analyte interactions in two ways: (a) the SARS-CoV-2 spike receptor-binding domain (RBD) is selected as an analyte and IgG or IgM is chosen as a probe ligand (b) mAbs (IgG/IgM) is selected as an analyte and the receptor binding domain is chosen as a ligand. The suggested sensor is unique in that it has great angular sensitivity and can detect the coronavirus virus quickly without producing a false-positive result. In ref. [20], a reference SPR analytical system which is home developed is presented, through which the effective coronavirus antigens detection was calculated using a fixed angle measurement mode with Protein A to achieve a greater sensitivity. The SPR system's performance has been enhanced by employing a reference region to prevent the refractivity inference of various solutions, and even to remove disruptions caused by non-specific absorptions. As a result, the reference SPR analytical system, which was developed in-house, has the potential to execute clinic diagnostics by immediately detecting crude patient samples without the need for pretreatment.

COVID-19 testing is currently performed using sluggish and costly technology. Techniques like enzyme-linked immunosorbent assay (ELISA), positron emission tomography (PET), and computed tomography (CT) are just a few examples of costly and time-consuming procedures that require well-trained personnel to perform. As previously discussed, the advantages of PCF over optical fibre and prism, therefore in this paper we proposed D-shape photonic crystal fibre–based SPR sensor for rapid coronavirus detection. The performance of the proposed sensor has been statistically evaluated using a variety of ligand- analytes, including antibodies-spike protein and spike protein-anti-spike protein. The simulation results are examined with COMSOL-multiphysics software. The finite element technique (FEM) is used to quantitatively examine the performance of proposed sensor.

The main objective of this paper is to propose a multilayer coated surface plasmon resonance PCF sensor for early detection of COVID-19. This multilayer sensor might assist minimise long detection procedures, clinical expenditures, and false-positive findings.

Proposed Sensors

In the proposed structure shown in Fig 1, the cladding contains two hexagon-shaped air-hole rings, and a small air hole in the middle. The central air hole is used for reducing the RI of the core mode, allowing for better phase matching between core and plasmonic modes [14]. For propagation of the core mode inside the fibre, two air hole rings are added. Diameter of the holes present inside the 2nd layer is somewhat larger than the hole's diameter in the 1st layer in order to reduce the refractive index of the cladding even further and improve core mode propagation. The ratio for air hole's diameter to hole-hole spacing of the air holes is determined for all of these designs such that confinement loss is increased and core mode propagation is maintained. The designed structure is built of silica, and all of the holes are filled with air. The following are the numerical values of

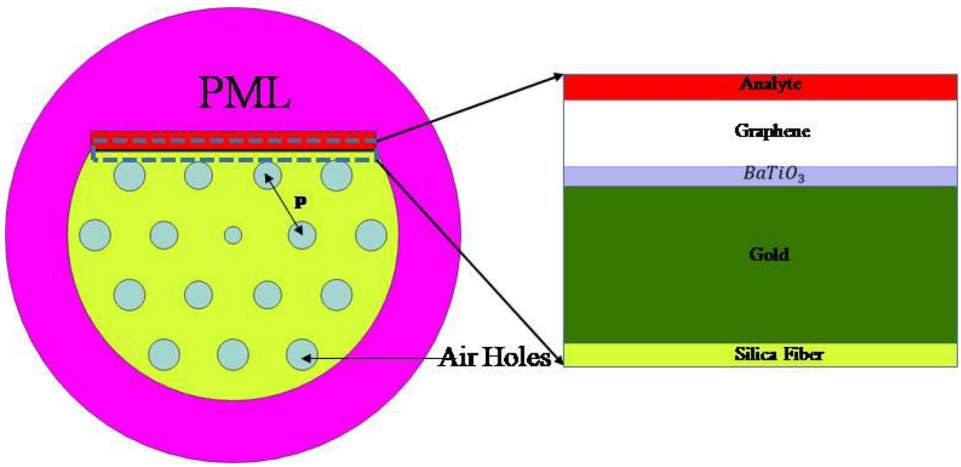

Fig. 1 D-shape photonic crystal fibre–based surface plasmon resonance biosensor

parameters: hole to hole spacing $p = 1.9\mu m$, RI of air holes $n_{air} = 1.0$, diameter of the centre air hole $d_c = 0.25p$, inner layer's air holes diameter $d_1 = 0.4p$, outer layer's air holes diameter $d_2 = 0.45p$, and thickness of gold plasmonic metal layer $t = 40nm$ [17]. The thickness of perfectly matched layer (PML) is employed as $0.9p$.

Gold nanomaterials having visible plasmon absorption cause their attractive and suitable applications in enhanced surface plasmon resonance (SPR) biosensors and optical sensing. In addition to that, a monolayer of barium titanate (BaTiO3) of thickness $5nm$ with RI of 2.4043 is used [21]. The dielectric characteristics of BaTiO3 increase the value of the refractive index with a little loss of electrons. As a result, BaTiO3 may produce a larger surface plasmon resonance wavelength changes with smaller refractive index change in the sensing medium. Furthermore, being a 2-dimensional substance, graphene improves sensitivity of the suggested sensor by ensuring good contact with the biological sample molecules because of its hexagonal shape ordered structure of carbon atoms. The graphene layer improves the interaction between the probe and the ligand. N graphene layers are present with each individual layer which is $0.34nm$ thick; overall graphene layer thickness is 0.34N. The following equation can be used to calculate graphene's refractive index.

$$n = 3 + i * C_1 * \lambda/3. \tag{1}$$

where $C_1 = 5.446\mu m^{-1}$ and λ is the wavelength of the vacuum. Five graphene layers are considered for optimization because the electronic characteristics of graphene alter as the no. of layers of graphene exceeds five. Single-layer graphene's electronic bands divide, and its infrared conductivity spectra converge on bulk graphite's behaviour [22, 23]. To fabricate this sensor, PCF can be fabricated by using stack and draw process [24] and different metals can be deposited inside the PCF by using the high-pressure CVD technique [25].

To identify the new coronavirus, the samples are taken of human blood or SARS-CoV-2 virus from nasopharyngeal swabs that contain monoclonal antibodies (IgG/IgM). As soon as possible after collecting the samples, they must be put in the viral transport medium (VTM) kit. A coronavirus 2 spike or monoclonal antibodies (IgG/IgM) can flow over the sensor surface as an analyte with phosphate-buffered saline (PBS). The suggested sensor can detect the SARS-CoV-2 in two ways: (a) the SARS-CoV-2 spike receptor-binding domain (RBD) is selected as an analyte and IgG or IgM is chosen as a probe ligand and (b) mAbs (IgG/IgM) is selected as an analyte and the receptor binding domain is chosen as a ligand. The probe ligand is bound on the layer of graphene in the sensing area through 1-pyrene-butyric acid n-hydroxy-succinimide ester (PBASE). In addition, due to the interaction of ligand-analyte binding, the refractive index of the sensing area is gradually rising. To realise the interaction mechanism of the SARS-CoV-2 spike RBD, a rate constant distribution (RCD) algorithm with AIDA was established in references [26, 27]. The real experimental interaction mechanism of SARS-CoV-2 spike RBD with human ACE2 is the same or almost similar to the algorithm [26]. The affinity constant (KD), association (ka), and dissociation (kd) rate constants are varied due to variation in ligands and analyte. Therefore, the rate constants value at the different concentration levels (concentration of 1.95 to 62.5 nM) of virus spike RBD is followed, as described in references [26–29]. The sensing region refractive index can be determined by the following equation:

$$n_{analyte} = n_{PBS} + C_a(\delta n/\delta c). \tag{2}$$

where $c_{analyte}$ is the concentration of of the target analyte, n_{PBS} is the concentration of the PBS solution with a RI of 1.3348, and $\delta n/\delta c = 0.181 cm^3/gm$ is the rate of change of RI modification in RI concentration. Furthermore, due to the interaction of the binding, Table 1 demonstrates that the RI steadily increases as the concentration increases [26–28, 30].

The experimental setup to detect the COVID-19 is shown in Fig. 2

Simulation, Results, and Discussion

The proposed sensor is simulated with the COMSOL multiphysics software with FEM method for x-polarised mode. The core mode and plasmonic mode of the sensor are analysed in 0.4 to 0.9 μm wavelength range. The monoclonal antibodies IgG/IgM must be immobilised on surface of graphene using PBASE to find the coronavirus-2 as ligand.

Table 1 RI of various concentrations for anti-spike's protein (IgG-H014) and coronavirus 2 spike RBD

SARC-CoV-2 spike with PBS (500nM) solution concentration (nM)	Change in RI of SARC-CoV-2 RBD solution	Concentration IgG with PBS (500nM) solution	Change in RI of IgG solution
0	0.00	0	0.00
1.953125	0.0023	1.74	0.0021
3.9065	0.0046	3.47	0.0043
7.8125	0.0069	6.94	0.0066
15.525	0.0093	13.9	0.0089
31.25	0.0117	21.8	0.0112
62.5	0.0143	-	-

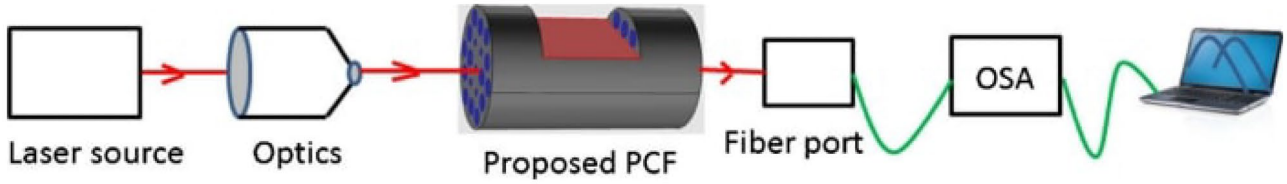

Fig. 2 Experimental setup to detect COVID-19 virus

Later, as an analyte, the binding interactions of ligand and the analyte change the RI in the used sensing medium. The refractive index of the sensing layer is calculated as $n_a = 1.3348 + \Delta n$ in the simulation, where RI of phosphate-buffered saline PBS (pH-7.4) is 1.3348, and Δn represents the variation in various binding concentrations of ligand and analyte in the sensing area. To solve the changing Δn and realise the coronavirus-2 viral spike RBD interaction mechanism, the rate-constant distribution (RCD) method with the adaptive interaction distribution algorithm (AIDA) is applied [19, 26–28]. The confinement loss (CL) of the PCF can be calculated as [31]:

$$\alpha(dB/cm) = 8.686 \times \frac{2\pi}{\lambda} Im(n_{eff}) \times 10^4, \tag{3}$$

where $Im(n_{eff})$ is imaginary part of mode index for operating wavelength $\lambda(\mu m)$. The performances of SPR sensors are characterised amplitude sensitivity, wavelength sensitivity (S_λ), and resolution (R), which are defined as [14]:

$$S_A(nm/RIU) = \Delta CL_p/\Delta n_a \times CL, \tag{4}$$

$$S_\lambda(nm/RIU) = \Delta\lambda_p/\Delta n_a, \tag{5}$$

$$R(RIU) = \Delta n_a \times \Delta\lambda_{min}/\Delta\lambda_{peak}, \tag{6}$$

where ΔCL is the difference in confinement loss peak amplitude. $\Delta\lambda_p$ is the shift in the resonant peak for Δn_a change in refractive index of analyte.

For the PBS solution, the phase of core mode and plasmonic mode match at 0.709 μm wavelength and thus the confinement loss maximises in the vicinity of this wavelength. Core mode, plasmonic mode, and phase matching are shown in Figs. 3, 4, and 5.

The confinement loss variation for RBD as an analyte is shown in Fig. 6 and peak values and their differences for different concentration of RBD analyte are shown in Table 2. The minimum threshold values of wavelength and CL for COVID detection will be (0 to 1.953125nM) 0.005μm and 3.1955dB/cm. So for the greater values of both wavelength and CL from threshold values, the sample will be COVID positive if both values are lesser then threshold then COVID negative and in other cases we have to try again. Similarly for

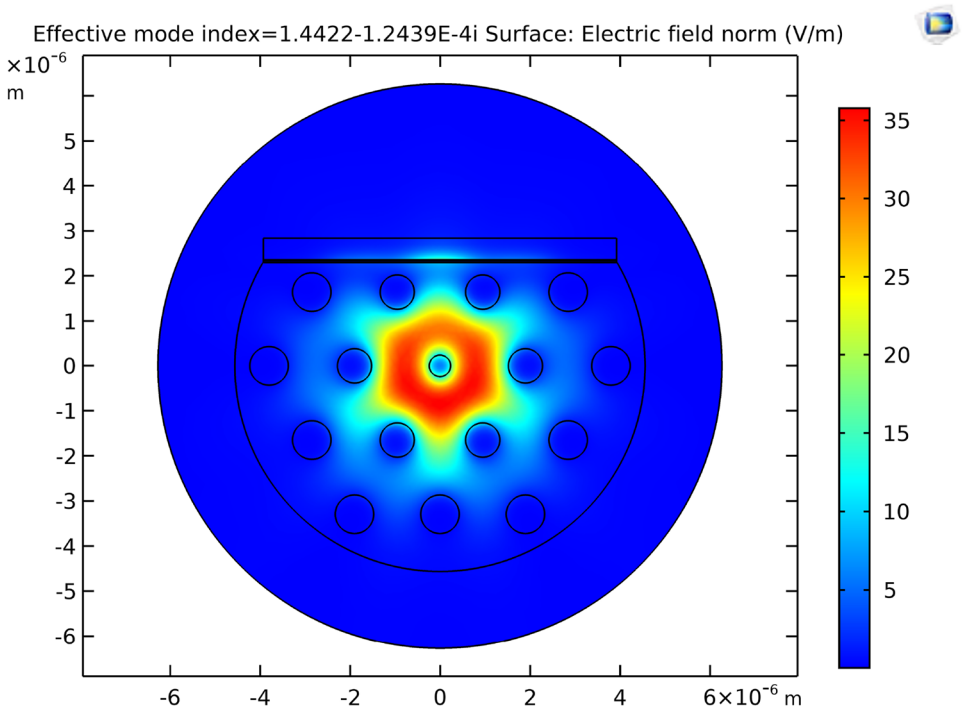

Fig. 3 Energy distribution of core mode at phase matching of core mode and plasmonic mode

Table 2 Sensing parameter at different SARS-CoV-2 virus spike RBD as an analyte

SARS-Cov-2 RBD concentration (ConRBD) with PBS (500 nM)	SPR wavelength	Maximum confinement loss	Change in SPR peaks	Change in confinement loss
0	0.72	99.6702	Ref	Ref
1.953125	0.725	102.8657	0.005	3.1955
3.9065	0.73	106.013	0.010	6.3428
7.8125	0.74	109.3452	0.02	9.675
15.525	0.745	112.8679	0.025	13.1977
31.25	0.755	116.3131	0.035	16.6429
62.5	0.76	119.9499	0.04	20.2797

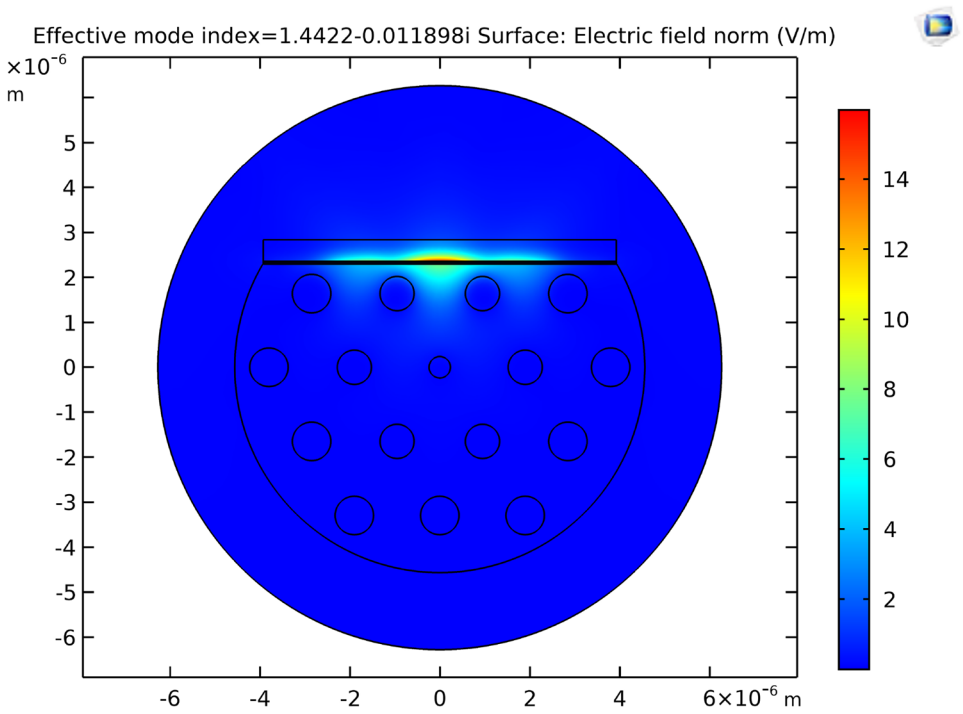

Fig. 4 Energy distribution of plasmonic mode at phase matching of core mode and plasmonic mode

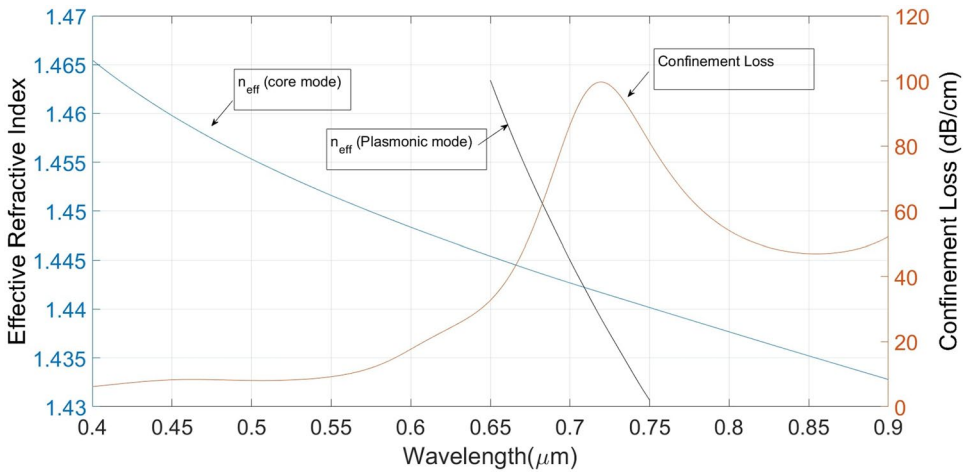

Fig. 5 Dispersion relation of proposed sensor at 1.3348 RI of PBS solution

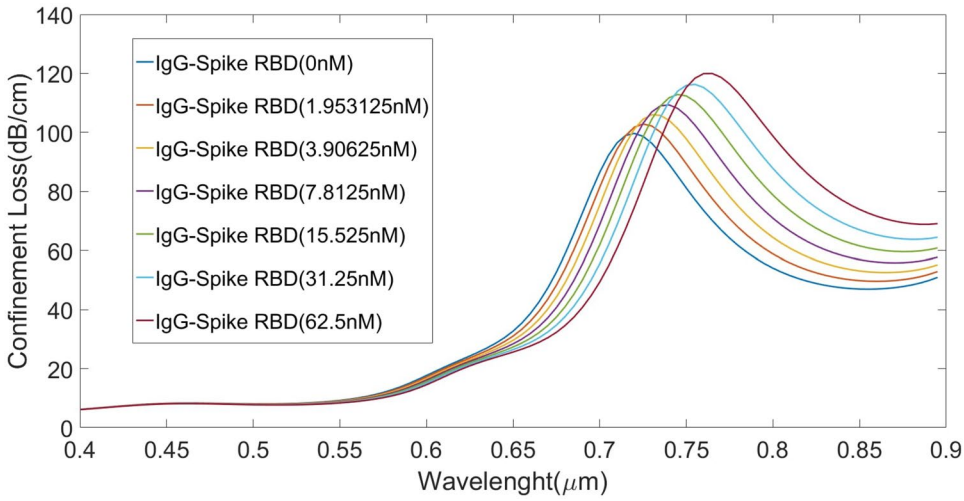

Fig. 6 Confinement loss variations of SPR-based sensor during the immobilisation of various SARS-CoV-2 virus spike RBD concentrations of 1.953125 to 62.5 nM

Table 3 Sensing parameter at different concentrations (0 to 27.8 nM) of anti-spike protein (IgG-H014) as an analyte

IgG concentration with PBS (500 nM)	SPR wavelength	Maximum confinement loss	Change in SPR peaks	Change in confinement loss
0	0.72	99.6702	Ref	Ref
1.74	0.725	102.5929	0.005	2.9227
3.47	0.73	105.6659	0.010	5.9957
6.94	0.74	108.8022	0.02	9.132
13.9	0.745	112.3033	0.025	12.6331
21.8	0.75	115.5298	0.03	15.8596

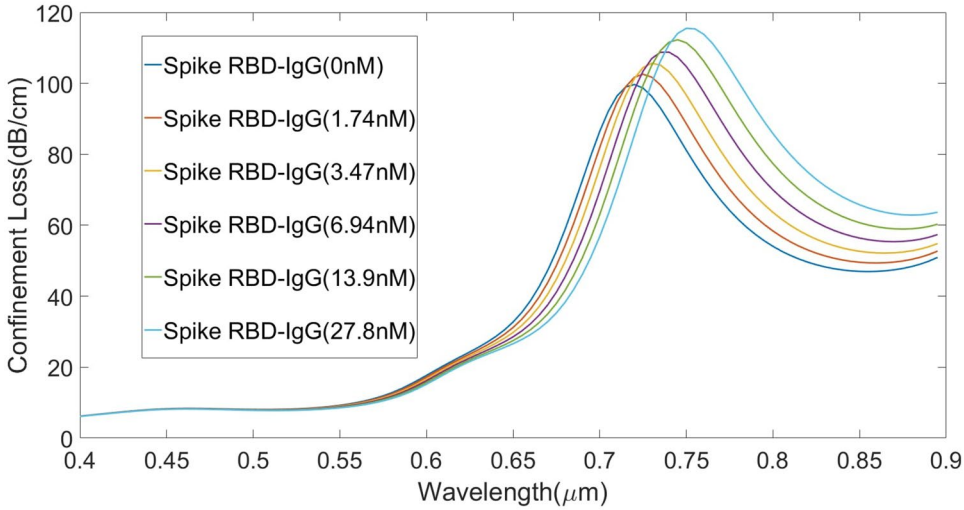

Fig. 7 Confinement loss variations of SPR-based sensor during the immobilisation of different concentrations (1.74 to 27.8 nM) of anti-spike protein (IgG-H014)

anti-spike protein as an analyte for different concentration, Cl variation and their differences are shown in Fig. 7 and Table 3. The minimum threshold values of wavelength and CL for COVID detection will be (0 to 1.74nM) 0.005μm and 2.9227dB/cm. The amplitude sensitivity, wavelength sensitivity, and resolution are calculated as 15.26/RIU, 2380nm/RIU, and 0.00042. The wavelength sensitivity of the given sensor is better than the sensor proposed in refs. [14–18].

Conclusion

A multi-layer covered surface plasmon resonance sensor for novel coronavirus early diagnosis is presented in this study. The amplitude sensitivity, wavelength sensitivity, and resolution are calculated as 15.26/RIU, 2380nm/RIU, and 0.00042. Due to to D-shape PCF, this sensor has reduced complexity over a prism-based sensor. The performance of the proposed sensor is also good which makes it a suitable candidate for COVID detection.

Acknowledgements The authors giving thanks to the Indian Institute of Information Technology Allahabad, Prayagraj, and MHRD — Government of India for providing the resources, infrastructure, and financial support.

Author Contribution Concept and design of the prototype experimental setup and analysis of results and preparation of the manuscript are done by Ankur Gupta. Akhilesh Tiwari has done the manuscript review. Data analysis is done by Tanu Singh and Rajat kumar Singh. All the authors have read and approved the final manuscript.

Data Availability The data that support the findings of this study are available from the corresponding author upon reasonable request.

Declarations

Ethical Approval Not applicable.

Conflict of Interest The authors declare no competing interests.

References

1. Huang C, Wang Y, Li X, Ren L, Zhao J, Yi H, Zhang L, Fan G, Jiuyang X, Xiaoying G, Cheng Z, Ting Y, Xia J, Wei Y, Wenjuan W, Xie X, Yin W, Li H, Liu M, Cao B (2020) Clinical features of patients infected with 2019 novel coronavirus in Wuhan, China. The Lancet 395:01
2. Wu J, Leung K, Leung G (2020) Nowcasting and forecasting the potential domestic and international spread of the 2019-nCoV outbreak originating in Wuhan, China: a modelling study. The Lancet 395:01
3. Cucinotta D, Vanelli M (2020) WHO declares COVID-19 a pandemic. Acta Bio-Medica: Atenei Parmensis 91:157–160
4. Asif M, Ajmal M, Ashraf G, Muhammad N, Aziz A, Iftikhar T, Wang J, Liu H (2020) The role of biosensors in coronavirus disease-2019 outbreak. Curr Opin Electrochem 23:174–184. (Electrocatalysis Sensors and Biosensors)
5. Hoehl S, Berger A, Kortenbusch M, Cinatl J, Bojkova D, Rabenau H, Behrens P, Böddinghaus B, Götsch U, Naujoks F, Neumann P, Schork J, Tiarks-Jungk P, Walczok A, Eickmann M, Vehreschild M, Kann G, Wolf T, Gottschalk R, Ciesek S (2020) Evidence of SARS-CoV-2 infection in returning travelers from Wuhan, China. N Engl J Med 382:02
6. Feiyun C, Zhou HS (2020) Diagnostic methods and potential portable biosensors for coronavirus disease 2019. Biosens Bioelectron 165
7. Rodovalho V, Alves L, Castro ACH, Madurro JM, Madurro A, Santos A (2015) Biosensors applied to diagnosis of infectious diseases - an update. Austin J Biosens Bioelectron 1:1–12
8. Saylan Y, Erdem Ö, Ünal S, Denizli A (2019) An alternative medical diagnosis method: Biosensors for virus detection. Biosensors 9:65
9. Berger CE, Greve J (2000) Differential SPR immunosensing. Sens Actuators B Chem 63(1–2):103–108
10. Liedberg B, Nylander C, Lunström I (1983) Surface plasmon resonance for gas detection and biosensing. Sens Actuators 4:299–304
11. Russell P (2003) Photonic crystal fibers. Science 299(5605):358–362
12. Sharma KK, Gupta A (2013) Log-periodic-type photonic crystal fiber structures and their propagation characteristics. Opt Eng 52(11):1–7
13. Jorgenson RC, Yee SS (1993) A fiber-optic chemical sensor based on surface plasmon resonance. Sens Actuators B Chem 12(3):213–220
14. Hassani A, Skorobogatiy M (2006) Design of the microstructured optical fiber-based surface plasmon resonance sensors with enhanced microfluidics. Opt Express 14:11616–11621
15. Gupta A, Anand H, Singh A, Singh RK, Tiwari A (2019) Photonic crystal fiber based surface plasmon resonance bio-sensors with bimetallic selectively filled metal layers. In 2019 Workshop on Recent Advances in Photonics (WRAP), p 1–3
16. Tian M, Lu P, Chen L, Lv C, Liu D (2012) All-solid d-shaped photonic fiber sensor based on surface plasmon resonance. Opt Commun 285(6):1550–1554
17. Gupta A, Gadia R, Singh A, Singh R, Tiwari A (2021) Design analysis of multi sample-single analyte surface plasmon resonance biosensor based on d-shape photonic crystal fiber
18. Gupta A, Singh H, Singh A, Singh RK, Tiwari A (2020) D-shaped photonic crystal fiber-based surface plasmon resonance biosensors with spatially distributed bimetallic layers. Plasmonics 18
19. Mostufa S, Akib TBA, Rana MM, Mehedi I, Al-Saggaf U, Alsaggaf A, Alsaggaf M, Alam MS (2022) A numerical approach to design the graphene-based multilayered surface plasmon resonance biosensor for the rapid detection of the novel coronavirus. OSA Continuum 1:494–515
20. Zain HA, Batumalay M, Harun SW (2021) Overview of surface plasmon resonance optical sensors for COVID-19 (SARS-CoV-2) detection. J Phys Conf Ser 2075:012009
21. Pal A, Jha A (2021) A theoretical analysis on sensitivity improvement of an spr refractive index sensor with graphene and barium titanate nanosheets. Optik 231:166378
22. Bruna M, Borini S (2009) Optical constants of graphene layers in the visible range. Appl Phys Lett 94:031901–031901
23. Dash J, Jha R (2015) On the performance of graphene-based d-shaped photonic crystal fibre biosensor using surface plasmon resonance. Plasmonics 10:02
24. Pysz D, Kujawa I, Stepien R, Klimczak M, Filipkowski A, Franczyk M, Kociszewski L, Buzniak J, Harasny K, Buczynski R (2014) Stack and draw fabrication of soft glass microstructured fiber optics. Bullet Polish Acad Sci Tech Sci 62:667–682
25. Sazio P, Amezcua-Correa A, Finlayson C, Hayes J, Scheidemantel T, Baril N, Jackson B, Won D-J, Zhang F, Margine E, Gopalan V, Crespi V, Badding J (2006) Microstructured optical fibers as high-pressure microfluidic reactors. Science (New York, N.Y.) 311:1583–1586

26. Forssén P, Samuelsson J, Lacki K, Fornstedt T (2020) Advanced analysis of biosensor data for SARS-CoV-2 RBD and ACE2 interactions. Anal Chem
27. Lan J, Ge J, Yu J et al (2020) Structure of the SARS-CoV-2 spike receptor-binding domain bound to the ACE2 receptor. Nature 581:215–220 (PMID: 32786452)
28. Forssén P, Multia E, Samuelsson J, Andersson M, Aastrup T, Altun S, Wallinder D, Wallbing L, Liangsupree T, Riekkola M-L, Fornstedt T (2018) Reliable strategy for analysis of complex biosensor data. Anal Chem 90(8):5366–5374 (PMID: 29589451)
29. Tian X, Li C, Huang A, Xia S, Lu S, Shi Z, Lu L, Jiang S, Yang Z, Wu Y, Ying T. Potent binding of 2019 novel coronavirus spike protein by a SARS coronavirus-specific human monoclonal antibody. Emerg Microbes Infect 9(1):382–385
30. Li Z, Yi Y, Luo X, Xiong N, Liu Y, Li S, Sun R, Wang Y, Hu B, Chen W, Zhang Y, Wang J, Huang B, Lin Y, Yang J, Cai W, Wang X, Cheng J, Chen Z, Ye F (2020) Development and clinical application of a rapid IgM-IgG combined antibody test for SARS-CoV-2 infection diagnosis. J Med Virol 92:02
31. Ferrarini D, Vincetti L, Zoboli M, Cucinotta A, Selleri S (2002) Leakage properties of photonic crystal fibers. Opt Express 10(23):1314–1319